Journal of Computational Applied Mechanics 2025, 56(2): 411-423

DOI: 10.22059/jcamech.2024.384209.1268

RESEARCH PAPER

Comparative study of the dynamic response between functionally graded sandwich plates and four-parameter FG plates

Messas Tidjani [a], Tamrabet Abdelkader [b], Bouhadra Abdelhakim [a,c,*], Menasria Abderahmane [a, c], Refrafi Salah [a], Mamen Belgacem [a], Ali Alselmi Nimer [d]

[a] *Department of Civil Engineering, Faculty of Science and Technology, Abbes Laghrour University, Khenchela 40000, Algeria*

[b] *Department of Civil Engineering, Faculty of Technology, University of Ferhat Abbas, Sétif 19137, Algeria*

[c] *Material and Hydrology Laboratory, Civil Engineering Department, Faculty of Technology, Djillali Liabes University, Sidi Bel Abbes 22000, Algeria*

[d] *Civil Engineering Department, College of Engineering, Jazan University, Jazan 114, Saudi Arabia*

Abstract

This paper presents an efficient higher-order theory for analyzing the dynamic behavior of two types of sandwich plates: functionally graded sandwich plates (FGSPs) and four-parameter functionally graded plates (FPFGPs). The FGSP consists of two functionally graded (FG) face sheets and a ceramic core. For FGSPs, the variation follows a power-law distribution, while for FPFGPs; it adheres to Tornabene's model. To ensure that transverse shear stresses vanish at the top and bottom surfaces of the FGSP, a trigonometric shear deformation theory is employed. This theory incorporates four displacement field variables with indeterminate integral terms. The governing equations are derived using Hamilton's principle and solved using the Navier solution method for simply supported boundary conditions. Validation results demonstrate excellent agreement between the proposed theory and existing literature. Additionally, a detailed parametric study highlights the influence of key geometric and mechanical parameters, including the power-law index, side-to-thickness ratio, and aspect ratio, on the dynamic behavior of the plates.

Keywords: Dynamic analysis, functionally graded materials, sandwich plates, four-parameter model, higher-order theory;

1. Introduction

Free vibration analysis is an essential area of study in structural mechanics. It involves investigating structures' natural frequencies and mode shapes when subjected to initial disturbances and allowing them to vibrate freely without external excitation. Understanding the behavior of structures under free vibration is crucial for designing and analysing various engineering systems. Different mathematical models and solution techniques have been employed to accurately predict the natural frequencies and mode shapes of FGM structures' free vibration analysis. Researchers have proposed various approaches, including variable kinematics models, unified solution methods,

* Corresponding author. Tel.: +213-77-718-9718;
E-mail address: abdelhakim.bouhadra@univ-khenchela.dz

shell theories, wavelet methods, and finite element methods [1-5].

Researchers conducted various investigations to assess the dynamic behaviors of FGMs shells by investigating the influence of multiple parameters, such as material gradation, boundary conditions, geometrical properties, and power law exponents, on FGM structures' natural frequencies and mode shapes. Neves et al.[6]analyzed the free vibration of FG shells using the Carrera unified formula merged with the radial basis function collocation method. Their results indicated that the fundamental frequency decreases with increased radii of curvature and power law exponent. [7] analyzed the buckling behavior of FG sandwich plate under the effect of porosity and foam distribution resting in Winkler–Pasternak elastic medium. Furthermore, [8] used different mathematical models to analyze the free vibration of FGM doubly curved shells. They reported that increasing the number of higher-order theories does not necessarily yield accurate results for natural frequencies. [9] employed the Haar Wavelet method to examine the free vibration of FGM shells and plates. They observed that the frequencies of FGM shells and plates have an inverse relation with the material exponent, length-to-radius ratio, and semi-vertex angle. [10] choose the transverse shear parabolic correction to fulfil the correct transverse shear strain energy. With a parabolic shear strain distribution imposed in the compatible strain part, the investigation of shell structure behavior has been performed based on enhanced solid-shell elements.

The free vibration analysis of FGM beams has also received significant attention. [11] study the dynamic behavior of FG porous beams embedded in Winkler–Pasternak elastic medium subjected to thermal shock using a novel numerical approach and consider the material properties to be temperature- and position-dependent. [12] have introduced a novel finite beam element for examining the free vibration characteristics of porous beams that exhibit a gradual variation in mechanical properties. The governing equations are derived using a mixed variational formulation and incorporate a new parabolic distribution of transverse shear strains. [13] studied the natural frequency of a non-uniform beam with lengthwise material distribution laying on a Winkler-Pasternak foundation model. The equations of motion for the beam have been obtained using the Euler-Bernoulli beam theory (EBBT), the Rayleigh-Ritz method, and the principle of Hamilton.

In analyzing the free vibration of functionally graded plates, several studies have been conducted to investigate the effects of various parameters on the natural frequencies.

[14] presented a comprehensive study of the free vibration characteristics of FGM plates partially submerged in a fluid. Four gradient types of continuously varying material properties are studied: power law, exponential, sinusoidal, and cosine, and based on the variational principle, the governing equations of the fluid-plate interaction system are derived. To solve the problem, the differential quadrature (DQ) method has been used.[15] used a new hybrid theory to analyze functionally graded plates' equilibrium, fundamental frequency, and stability. The equations of motion are derived using the Hamilton principle and solved using the Navier-type solution for the case of simply supported boundary conditions. In 2023, [16] investigated the equilibrium, the dynamic, and the stability of two-layer functionally graded material (FGM) plates, including shear connectors and resting on elastic foundations, by using the combination of Navier's solution based on nth-order shear deformation plate theory and finite element method.

The main objective of this study is to use a new displacement field containing fewer unknowns compared to other quasi-3D shear deformation theories. This model simplifies the problem and considers the effect of transverse stretching, which is not considered in the case of 2D-shear deformation theories.

Moreover, a more comprehensive study examined the result of many parameters on natural frequencies, including the side-to-thickness ratio, thickness ratio, aspect ratio, volume fraction index, and material properties. Finally, numerical results are verified by comparisons with other plates' theories' solutions found in the literature to ensure the accuracy and effectiveness of the current approaches. The present findings contribute to understanding the behavior of functionally graded plates under free vibration conditions and provide valuable insights for design and optimization purposes.

2. Mathematical modeling

2.1. Kinematics Structural Definition

In the current studies, we consider single layer plate [FP-FGM] with uniform thickness (h), length (a), and width (b) and multilayer plate [P-FGSP] composed of three layers. The middle layer is pure ceramic and their face sheets are FGM. The (x, y) coordinates are the in-plane directions and z according to thickness direction, see Fig. 1.

The material proprieties of the FGM plate are stated as:

$$P(z) = P_m + \left(P_c - P_m\right)V\left(z\right) \tag{01}$$

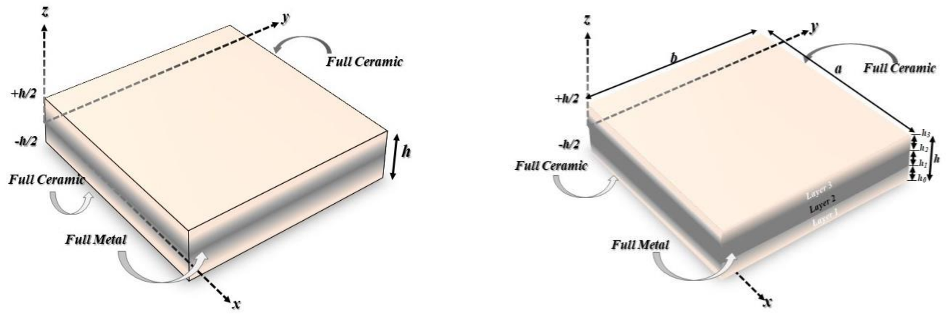

a) FP-FGM b) P-FGSP

Figure 1: Coordinate system and geometry of FGM plate.

The volume fraction is given by:
Functionally graded sandwich plate [PFGSP]:

$$\begin{aligned}
&V^{(1)}(z)=\left(\frac{z-h_0}{h_1-h_0}\right)^k && h_0\le z\le h_1\\
&V^{(2)}(z)=1 && h_1\le z\le h_2\\
&V^{(3)}(z)=\left(\frac{z-h_3}{h_2-h_3}\right)^k && h_2\le z\le h_3
\end{aligned} \tag{02}$$

Four-parameter model [FPM] given as[17]:

$$V(z)=\left(1-a\left(\frac{1}{2}-\frac{z}{h}\right)+b\left(\frac{1}{2}-\frac{z}{h}\right)^c\right)^k \tag{03}$$

Where k is the volume fraction index ($0\le k\le\infty$) which indicates the material variation profile through the FGSP structure.
The next figures represent the variations of Young's modulus through the thickness for different values of the three parameters a, b, c and the power-law index "k":

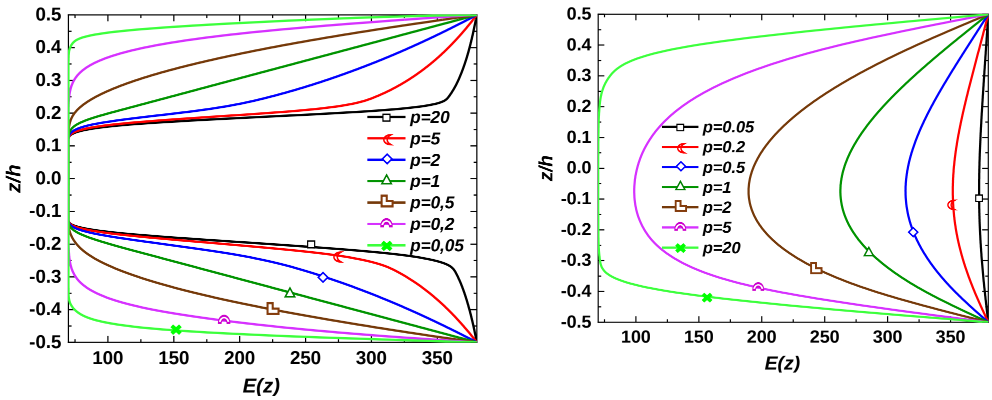

a) P-FGSP b) FPM-FGM (a=1/b=1/c=3)

Figure 2: The variation of Young modulus E(z) across the thickness versus the material index "k".

2.2. Kinematic and constitutive relations

The displacement field retained in the present work can be described as:

$$\begin{aligned} u(x,y,z,t) &= u_0(x,y,t) - z w_{0,x} + k_1\, A'\, f(z)\theta_{,x}(x,y,t) \\ v(x,y,z,t) &= v_0(x,y,t) - z w_{0,y} + k_2\, B'\, f(z)\theta_{,y}(x,y,t) \\ w(x,y,z,t) &= w_0(x,y,t) + g(z)\varphi_z(x,y,t) \end{aligned} \tag{04}$$

The shape function $f(z)$ is proposed as:

$$f(z) = \frac{z}{\pi}\left(1 - \frac{5\pi^2}{37}\left(\frac{z}{h}\right)^2\right), \quad g(z) = \frac{\partial f(z)}{\partial z} \tag{05}$$

The strain relations according to the displacement field are given as:

$$\begin{aligned} &\begin{Bmatrix} \varepsilon_x \\ \varepsilon_y \\ \gamma_{xy} \end{Bmatrix} = \begin{Bmatrix} u_{0,x} \\ v_{0,y} \\ u_{0,y} + v_{0,x} \end{Bmatrix} - z \begin{Bmatrix} w_{0,xx} \\ w_{0,yy} \\ 2w_{0,xy} \end{Bmatrix} + \\ &f(z) \begin{Bmatrix} k_1\theta \\ k_2\theta \\ k_1 A'\theta_{,xy}(x,y,t) + k_2 B'\theta_{,yx}(x,y,t) \end{Bmatrix}, \\ &\begin{Bmatrix} \gamma_{yz} \\ \gamma_{xz} \end{Bmatrix} = g(z) \begin{Bmatrix} k_2\, A'\theta_{,x}(x,y,t) + \varphi_{z,y} \\ k_1 A'\theta_{,y}(x,y,t) + \varphi_{z,x} \end{Bmatrix}, \\ &\varepsilon_z = g'(z)\ \varepsilon_z^0 \end{aligned} \tag{06}$$

$$k_1 = \lambda^2, \qquad k_2 = \mu^2, \quad A = -\frac{1}{\lambda^2}, \quad B = -\frac{1}{\mu^2} \tag{6a}$$

Where:

$$\lambda = \frac{m\pi}{a}, \qquad \mu = \frac{n\pi}{b} \tag{6b}$$

2.3. Constitutive relations

For the n^th layer, the linear constitutive relations of FGSP are given as:

$$\{\sigma_i\} = \left[C_{ij}\right]\{\varepsilon_j\} \tag{08a}$$

$$C^{(n)}{}_{11} = C^{(n)}{}_{22} = C^{(n)}{}_{33} = \frac{(1-\nu)E^{(n)}(z)}{(1-2\nu)(1+\nu)},$$
$$C_{12}^{(n)} = C_{13}^{(n)} = C_{23}^{(n)} = \frac{\nu E^{(n)}(z)}{(1-2\nu)(1+\nu)}, \tag{08b}$$
$$C_{44}^{(n)} = C_{55}^{(n)} = C_{66}^{(n)} = \frac{E^{(n)}(z)}{2(1+\nu)}$$

2.4. Equations of motion

Hamilton's rule is used herein to derive the equations of motion and can be stated in analytical form as:

$$\int_0^T (\delta U + \delta V) dt = 0 \tag{09}$$

Where: δU is the variation of strain energy and δK is the variation of kinetic energy.
The variation of strain energy of the plate is calculated by:

$$\begin{aligned}\delta U = &\int_{-h/2}^{h/2} \int_A [\sigma_x \delta\varepsilon_x + \sigma_y \delta\varepsilon_y + \sigma_z \delta\varepsilon_z + \tau_{xy} \delta\gamma_{xy} \\ &+ \tau_{yz}\delta\gamma_{yz} + \tau_{xz}\delta\gamma_{xz}] dAdz \\ = &\int_A [N_x \delta\varepsilon_x^0 + N_y \delta\varepsilon_y^0 + N_z \delta\varepsilon_z^0 + N_{xy}\delta\gamma_{xy}^0 \\ &+ M_x^b \delta k_x^b + M_y^b \delta k_y^b + M_{xy}^b \delta k_{xy}^b + M_x^s \delta k_x^s \\ &+ M_y^s \delta k_y^s + M_{xy}^s \delta k_{xy}^s + S_{yz}^S \delta\gamma_{yz} + S_{xz}^S \delta\gamma_{xz}] dA = 0\end{aligned} \tag{10}$$

Where A is the surface; and stress resultants N, M, and Q are defined by

$$\begin{bmatrix} N_x & N_y & N_{xy} \\ M_x & M_y & M_{xy} \\ P_x & P_y & P_{xy} \end{bmatrix} = \sum_{n=1}^{3} \int_{h_n}^{h_{n+1}} (\sigma_x, \sigma_y, \tau_{xy}) \begin{Bmatrix} 1 \\ z \\ f(z) \end{Bmatrix} dz, \tag{11a}$$

$$(Q_{xz}, Q_{yz}) = \sum_{n=1}^{3} \int_{h_n}^{h_{n+1}} (\tau_{xz}, \tau_{yz}) \frac{\partial f(z)}{\partial z} dz$$

$$N_z = \sum_{n=1}^{n=3} \int_{hn}^{h_{n+1}} \sigma_z \ \mathrm{g'(z)}\, dz\,, \quad (S_{xz}^s, S_{yz}^s) = \sum_{n=1}^{n=3} \int_{hn}^{h_{n+1}} (\tau_{xz}, \tau_{yz}) \ \mathrm{g(z)}\, dz \tag{11b}$$

The variation of kinetic energy of the plate can be written as:

$$\delta K=\int_{-h/2}^{h/2}\int_A[\dot{u}\delta\dot{u}+\dot{v}\delta\dot{v}+\dot{w}\delta\dot{w}]\,\rho(\mathrm{z})dA\,dz=$$
$$\int_A\{I_0[\dot{u}_0\delta\dot{u}_0+\dot{v}_0\delta\dot{v}_0+\dot{w}_0\delta\dot{w}_0]$$
$$-I_1[\dot{u}_0\frac{\partial\delta\dot{w}_0}{\partial x}+\dot{v}_0\frac{\partial\delta\dot{w}_0}{\partial y}+\frac{\partial\dot{w}_0}{\partial x}\delta\dot{u}_0+\frac{\partial\dot{w}_0}{\partial y}\delta\dot{v}_0]+$$
$$I_2[\frac{\partial\dot{w}_0}{\partial x}\frac{\partial\delta\dot{w}_0}{\partial x}+\frac{\partial\dot{w}_0}{\partial y}\frac{\partial\delta\dot{w}_0}{\partial y}]$$
$$-J_1[\dot{u}_0\frac{\partial\delta\dot{\theta}}{\partial x}+\frac{\partial\dot{\theta}}{\partial x}\delta\dot{u}_0+\dot{v}_0\frac{\partial\delta\dot{\theta}}{\partial y}+\frac{\partial\dot{\theta}}{\partial y}\delta\dot{v}_0]+ \tag{12}$$
$$J_2[\frac{\partial\dot{w}_0}{\partial x}\frac{\partial\delta\dot{\theta}}{\partial x}+\frac{\partial\dot{\theta}}{\partial x}\frac{\partial\delta\dot{w}_0}{\partial x}+\frac{\partial\dot{w}_0}{\partial y}\frac{\partial\delta\dot{\theta}}{\partial y}+\frac{\partial\dot{\theta}}{\partial y}\frac{\partial\delta\dot{w}_0}{\partial y}]$$
$$+K_2[\frac{\partial\dot{\theta}}{\partial x}\frac{\partial\delta\dot{\theta}}{\partial x}+\frac{\partial\dot{\theta}}{\partial y}\frac{\partial\delta\dot{\theta}}{\partial y}]+J_1^s[\dot{w}_0\delta\dot{\varphi}_z+\dot{\varphi}_z\delta\dot{w}_0]$$
$$+K_2^s\dot{\varphi}_z\delta\dot{\varphi}_z\}dA$$

Where dot-superscript convention indicates the differentiation with respect to the time variable t; and (I0, I1,J1,I2,J2,K2,K2s) are mass inertias defined as:

$$(I_0,I_1,J_1,J_1^s,I_2,J_2,K_2,K_2^s)=$$
$$\sum_{n=1}^{n=3}\int_{hn}^{h_{n+1}}(1,z,f,g,z^2,zf,f^2,g^2)\rho(\mathrm{z})\,dz \tag{13}$$

Substituting the expressions of δU and δK from Eqs (10) and (12) into Eq. (19), and by simple mathematical technics, the following equations are obtained:

$$\delta u_0: N_{x,x}+N_{xy,y}=I_0\ddot{u}_0-I_1\ddot{w}_{0,x}-J_1\ddot{\theta}_{,x} \tag{14a}$$
$$\delta v_0: N_{xy,x}+N_{y,y}=I_0\ddot{v}_0-I_1\ddot{w}_{0,y}-J_1\ddot{\theta}_{,y} \tag{14b}$$
$$\delta w_0: M^b_{x,xx}+2M^b_{xy,xy}+M^b_{y,yy}=$$
$$I_0(\ddot{w}_0+\ddot{\theta})+I_1(\ddot{u}_{0,x}+\ddot{v}_{0,y})- \tag{14c}$$
$$I_2\nabla^2\ddot{w}_0-J_2\ddot{\theta}+J_1^s\ddot{\varphi}$$
$$\delta\theta: -k_1M^s_x-k_2M^s_y-\left(k_1A'+k_2B'\right)M^s_{xy,xy}$$
$$+k_1A'S^s_{xz,x}+k_2B'S^s_{yz,y}=I_0(\ddot{w}_0+\ddot{\theta})+ \tag{14d}$$
$$J_1(\ddot{u}_{0,x}+\ddot{v}_{0,y})-J_2\nabla^2\ddot{w}_0-K_2\ddot{\theta}+J_1^s\ddot{\varphi}$$
$$\delta\varphi_z: S^s_{xz,x}+S^s_{yz,y}-N_z=J_1^s(\ddot{w}_0+\ddot{\theta})+K_2^s\ddot{\varphi} \tag{14e}$$

By substituting Eq.(6) into Eq.(7), the resulting equation into Eq.(14). The equations of motion in terms of unknown's (δu0, δv0, δw0, δθ) are given by:

$$\begin{aligned}&A_{11}u_{0,xx}+A_{12}v_{0,xy}+A_{66}\left(u_{0,yy}+v_{0,xx}\right)-\\&B_{11}w_{0,xxx}-B_{12}w_{0,xyy}\ \ -2B_{66}w_{0,xyy}+B_{11}^{s}A'k_{1}\theta_{,xxx}\\&B_{12}^{s}B'k_{2}\theta_{,xyy}+B_{66}^{s}\left(A'k_{1}+B'k_{2}\right)\theta_{,xyy}+L\varphi_{z,x}\\&=I_{0}\ddot{u}_{0}-I_{1}\ddot{w}_{0,x}-J_{1}\ddot{\theta}_{,x}\end{aligned}\tag{15a}$$

$$\begin{aligned}&A_{12}u_{0,xy}^{1}+A_{22}v_{0,yy}^{1}+A_{66}\left(u_{0,xy}^{1}+v_{0,xx}^{1}\right)-B_{12}w_{0,xxy}^{1}\\&-B_{22}w_{0,yyy}^{1}-2B_{66}w_{0,xxy}^{1}+B_{12}^{s}A'k_{1}\theta^{1}{}_{,xxy}\\&B_{22}^{s}B'k_{2}\theta^{1}{}_{,yyy}+B_{66}^{s}\left(A'k_{1}+B'k_{2}\right)\theta^{1}{}_{,xxy}+L\varphi_{z,y}\\&=I_{0}\ddot{v}_{0}-I_{1}\ddot{w}_{0,y}-J_{1}\ddot{\theta}_{,y}\end{aligned}\tag{15b}$$

$$\begin{aligned}&B_{11}u_{0,xxx}+B_{12}\left(u_{0,xyy}+v_{0,xxy}\right)+B_{22}v_{0,yyy}+\\&2B_{66}\left(u_{0,xyy}+v_{0,xxy}\right)-D_{11}w_{0,xxxx}-2D_{12}w_{0,xxyy}\\&-D_{22}w_{0,yyyy}-4D_{66}w_{0,xxyy}+D_{11}^{s}A'k_{1}\theta_{,xxxx}+\\&D_{12}^{s}\left(A'k_{1}+B'k_{2}\right)\theta_{,xxyy}+D_{22}^{s}B'k_{2}\theta_{,yyyy}\\&+2D_{66}^{s}\left(A'k_{1}+B'k_{2}\right)\theta_{,xxyy}+L^{a}(\varphi_{z,xx}+\varphi_{z,yy})\\&=I_{0}(\ddot{w}_{0}+\ddot{\theta})+J_{1}(\ddot{u}_{0,x}+\ddot{v}_{0,y})-J_{2}\ddot{w}_{0,xxyy}-\\&K_{2}\ddot{\theta}_{,xxyy}+J_{1}^{s}\ddot{\varphi}\end{aligned}\tag{15c}$$

$$\begin{aligned}&-B_{11}^{s}A'k_{1}u_{0,xxx}-B_{12}^{s}\left(A'k_{1}v_{0,xxy}+B'k_{2}u_{0,xyy}\right)-\\&B_{22}^{s}B'k_{2}v_{0,yyy}-B_{66}^{s}\begin{pmatrix}\left(A'k_{1}+B'k_{2}\right)u_{0,xyy}\\+\left(A'k_{1}+B'k_{2}\right)v_{0,xxy}\end{pmatrix}\\&+D_{11}^{s}A'k_{1}w_{0,xxxx}+D_{12}^{s}\left(A'k_{1}+B'k_{2}\right)w_{0,xxyy}+\\&D_{22}^{s}B'k_{2}w_{0,yyyy}+2D_{66}^{s}\left(A'k_{1}+B'k_{2}\right)w_{0,xxyy}\\&-H_{11}^{s}\left(A'k_{1}\right)^{2}\theta_{,xxxx}\frac{\partial^{4}}{\partial x^{4}}-2H_{12}^{s}A'k_{1}B'k_{2}\theta_{,xxyy}-\\&H_{22}^{s}\left(B'k_{2}\right)^{2}\theta^{1}{}_{,yyyy}-H_{66}^{s}\left(A'k_{1}+B'k_{2}\right)^{2}\theta_{,xxyy}\\&+A_{44}^{s}\left(A'k_{1}\right)^{2}\theta_{,xx}+A_{55}^{s}\left(B'k_{2}\right)^{2}\theta_{,yy}+R(\varphi_{z,xx}+\varphi_{z,yy})\\&+A_{44}^{s}\varphi_{z,xx}+A_{55}^{s}\varphi_{z,yy}\\&=I_{0}(\ddot{w}_{0}+\ddot{\theta})+J_{1}(\ddot{u}_{0,x}+\ddot{v}_{0,y})-J_{2}\ddot{w}_{0,xxyy}-K_{2}\ddot{\theta}_{,xxyy}+J_{1}^{s}\ddot{\varphi}\end{aligned}\tag{15d}$$

$$\begin{aligned}&L(u_{0,x}+v_{0,y})-L^{a}(w_{0,xx}+w_{0,yy})-(R+A_{44}^{s})\theta_{,xx}\\&-(R+A_{55}^{s})\theta_{,yy}+R^{a}\varphi-A_{44}^{s}\varphi_{z,xx}-A_{55}^{s}\varphi_{z,yy}\\&=J_{1}^{s}(\ddot{w}_{0}+\ddot{\theta})+K_{2}^{s}\ddot{\varphi}\end{aligned}\tag{15e}$$

Where:

$$\left\{L \quad L^a \quad R \quad R^a\right\} = \sum_{n=1}^{n=3} \int_{hn}^{h_{n+1}} \lambda(z)\left\{1 \quad z \quad f(z) \quad f(z)\right\} g'(z)dz \tag{16}$$

$$\begin{Bmatrix} A_{11} & B_{11} & D_{11} & B_{11}^s & D_{11}^s & H_{11}^s \\ A_{12} & B_{12} & D_{12} & B_{12}^s & D_{12}^s & H_{12}^s \\ A_{66} & B_{66} & D_{66} & B_{66}^s & D_{66}^s & H_{66}^s \end{Bmatrix} = \sum_{n=1}^{n=3} \int_{hn}^{h_{n+1}} \lambda(z)\left[1, z, z^2, f(z), z\, f(z), f^2(z)\right] \begin{Bmatrix} \frac{1-\nu}{\nu} \\ 1 \\ \frac{1-2\nu}{2\nu} \end{Bmatrix} dz \tag{17}$$

$$A_{44}^s = A_{55}^s = \sum_{n=1}^{n=3} \int_{hn}^{h_{n+1}} \mu(z)\ [\mathrm{g}(z)]^2 dz \tag{18}$$

$$(A_{22},\ B_{22},\ D_{22},\ B_{22}^s,\ D_{22}^s,\ H_{22}^s) = (A_{11},\ B_{11},\ D_{11},\ B_{11}^s,\ D_{11}^s,\ H_{11}^s) \tag{19}$$

3. Solution procedure

The boundary conditions taken in the present work concerns those of simply supported edges and imposed like:

$$v_0 = w_0 = \theta = \theta_{,y} = \varphi = N_x = M_x^b = M_x^s = 0 \quad \text{at } x=0, a \tag{20a}$$

$$u_0 = w_0 = \theta = \theta_{,x} = \varphi = N_y = M_y^b = M_y^s = 0 \quad \text{at } y=0, b \tag{20b}$$

Based on the Navier type techniques, the following form for u0, v0, w0, and θ that satisfies the boundary conditions given in Eq. (20):

$$\begin{Bmatrix} u_0 \\ v_0 \\ w_0 \\ \theta \\ \varphi^z \end{Bmatrix} = \sum_{m=1}^{\infty}\sum_{n=1}^{\infty} \begin{Bmatrix} U_{mn} e^{iwt} \cos(\lambda\, x)\sin(\mu\, y) \\ V_{mn} e^{iwt} \sin(\lambda\, x)\cos(\mu\, y) \\ W_{mn} e^{iwt} \sin(\lambda\, x)\sin(\mu\, y) \\ X_{mn} e^{iwt} \sin(\lambda\, x)\sin(\mu\, y) \\ \Phi_{mn} e^{iwt} \sin(\lambda\, x)\sin(\mu\, y) \end{Bmatrix} \tag{21}$$

U_{mn}, V_{mn}, W_{mn}, X_{mn} and Φ_{mn} are arbitrary parameters and λ, μ are definite as:

$$\lambda = m\pi / a \ \text{ And } \ \mu = n\pi / b \tag{22}$$

Substituting Eq. (21) into Eq. (15), the analytical solutions can be gotten form:

$$\left(\left[a\right] - \omega^2\left[m\right]\right)\left\{U_{mn} \quad V_{mn} \quad W_{mn} \quad X_{mn} \quad \Phi_{mn}\right\} = \left\{0\right\} \tag{23}$$

ω is the is the fundamental frequency In witch:

$$a_{11}=-(A_{11}\alpha^2+A_{66}\beta^2)\,,\; a_{12}=-\alpha\;\beta\;\left(A_{12}+A_{66}\right),$$
$$a_{13}=\alpha(B_{11}\alpha^2+(B_{12}+2B_{66})\beta^2)$$
$$a_{14}=-\alpha(B_{11}^s A'k_1\alpha^2+B_{12}^s B'k_2\beta^2$$
$$+B_{66}^s\left(A'k_1+B'k_2\right)\beta^2)$$
$$a_{15}=L\alpha\,,\; a_{22}=-\alpha^2 A_{66}-\beta^2 A_{22}\,,$$
$$a_{23}=\beta(B_{22}\beta^2+(B_{12}+2B_{66})\alpha^2)$$
$$a_{24}=-\beta\begin{pmatrix} B_{22}^s B'k_2\beta^2+ \\ \alpha^2\left(B_{12}^s A'k_1+B_{66}^s\left(A'k_1+B'k_2\right)\right)\end{pmatrix}$$
$$a_{25}=L\beta\,,$$
$$a_{33}=-\alpha^2\left(D_{11}\alpha^2+\left(2D_{12}+4D_{66}\right)\beta^2\right)-D_{22}\beta^4 \tag{24}$$
$$a_{34}=D_{11}^s A'k_1\alpha^4+D_{12}^s\left(A'k_1+B'k_2\right)\beta^2\alpha^2$$
$$+D_{22}^s B'k_2\beta^4+2D_{66}^s\left(A'k_1+B'k_2\right)\beta^2\alpha^2$$
$$a_{35}=-L^a(\alpha^2+\beta^2)$$
$$a_{44}=-(2(k_1\beta^2 H_{66}^s+H_{66}^s\alpha^2 k_2)$$
$$+k_1(H_{11}^s\alpha^2+\beta^2 H_{12}^s+A_s^{44})$$
$$+k_2(\beta^2 H_{22}^s+A_s^{55}+H_{12}^s\alpha^2))$$
$$a_{45}=-[A_{44}^s\alpha^2+A_{55}^s\beta^2+R(\alpha^2+\beta^2)]\,,\; a_{55}=-(A_{44}^s\alpha^2+A_{55}^s\beta^2+R^a)$$
$$a_{12}=a_{21},\; a_{13}=a_{31},\; a_{14}=a_{41},\; a_{15}=a_{51}$$
$$a_{23}=a_{32},\; a_{24}=a_{42},\; a_{25}=a_{52}$$
$$a_{34}=a_{43},\; a_{35}=a_{53},\; a_{45}=a_{54}$$

And

$$m_{11}=m_{22}=-I_0\,,\; m_{13}=\alpha I_1\,,\; m_{14}=\alpha J_1\,,$$
$$m_{23}=\beta I_1\,,\; m_{24}=\beta J_1\; m_{35}=m_{45}=-J_1^s$$
$$m_{33}=-[I_0+I_2(\alpha^2+\beta^2)]\,,$$
$$m_{34}=-[I_0+J_2(\alpha^2+\beta^2)]\,, \tag{25}$$
$$m_{44}=-[I_0+K_2(\alpha^2+\beta^2)]$$
$$m_{55}=-K_2^s$$

Non-dimensional parameters:

$$\bar{\beta}=\omega a^2/\pi^2\sqrt{\rho h/D}\,,$$
$$D=Eh^3\Big/\left(12\left(1-\nu^2\right)\right), \tag{26}$$
$$\bar{\varpi}=\omega h\sqrt{\rho_m/E_m}$$

4. Numerical results

4.1. Comparative study

The first section presents two numerical examples of a simply supported FG plate under free vibration. The presented model has been first validated through the comparison with the existing data available. Two types of FGMs plates are considered: Al/Al2O3 and Al/ZrO2. The material properties of the FG plates are stated in Table 1.

Table 1: Material proprieties used in the FG plates

Proprieties	Metal		Ceramic		
	(Al)	*(Al)**	*(Al_2O_3)*	*(ZrO_2)*	*(ZrO_2)**
E (Gpa)	70	68.9	380	200	211
ν	0.3	0.33	0.3	0.3	0.33
P (kg/m^3)	2702	2700	3800	5700	4500

For the validation of the current model, a comparison study of the non-dimensional fundamental frequency is realized for an FG rectangular plate. As an initial example, a square (Al/Al2O3) plate with a thickness ratio of 5 to 20 and a power-law index of 0 to 10 is performed using various plate theories. The non-dimensional fundamental frequencies predicted by Sekkal et al. [18] and Abualnour et al. [19] and the current theory are compared in **Table 2**. It can be concluded that the results attained from the present model are closer to those of the proposed models.

Table 2: Non-dimensional fundamental frequency ω¯of (Al / Al2O3) square plates. Material proprieties used in the FG plates a) P-FGSP, b) FP-FGM.

	Mode *(m,n)*	Method	Power law index (*k*)				
			0	0.5	1	4	10
a/h	1(1,1)	Sekkal et al.[18] $\varepsilon_z \neq 0$	0.2130	0.1834	0.1665	0.1411	0.1321
		Abualnour et al.[19] $\varepsilon_z \neq 0$	0.2126	0.1829	0.1663	0.1411	0.1320
		Present $\varepsilon_z \neq 0$	0.2124	0.1828	0.1661	0.1411	0.1321
	2(1,2)	Sekkal et al. [18] $\varepsilon_z \neq 0$	0.4682	0.4064	0.3692	0.3052	0.2818
		Abualnour et al. [19] $\varepsilon_z \neq 0$	0.4674	0.4052	0.3687	0.3052	0.2817
		Present $\varepsilon_z \neq 0$	0.4661	0.4044	0.3677	0.3051	0.2814
	1(1,1)	Sekkal et al. [18] $\varepsilon_z \neq 0$	0.0578	0.0492	0.0443	0.0381	0.0364
		Abualnour et al. [19] $\varepsilon_z \neq 0$	0.0579	0.0495	0.0450	0.0390	0.0369
		Present $\varepsilon_z \neq 0$	0.0579	0.0495	0.0450	0.0390	0.0369
	2(1,2)	Sekkal et al. [18] $\varepsilon_z \neq 0$	0.1381	0.1180	0.1063	0.0905	0.0859
		Abualnour et al. [19] $\varepsilon_z \neq 0$	0.1383	0.1186	0.1078	0.0924	0.0868
		Present $\varepsilon_z \neq 0$	0.1383	0.1186	0.1078	0.0924	0.0869

4.2. Benchmark results

Next, parametric studies have been performed, and typical results are shown in Figures 3-6. **Figure. 3a** and **3b** depict the variation of the non-dimensional fundamental frequency of the FG sandwich plate and four parameters model plate. In **Figure. 3a**, the frequencies changes versus the aspect ratios. Although rapid decreasing of the frequencies when a/b increased and then they had relative values before a/b=3, **Figure. 3b** shows the variation of non-dimensional fundamental frequency versus index k, so with the increase of the power law index k, the frequencies are decreasing, which means the stiffness of the plate reduced when the metal is including. The sandwich configuration 1-2-1 is closer to the other configurations' four-parameter model.

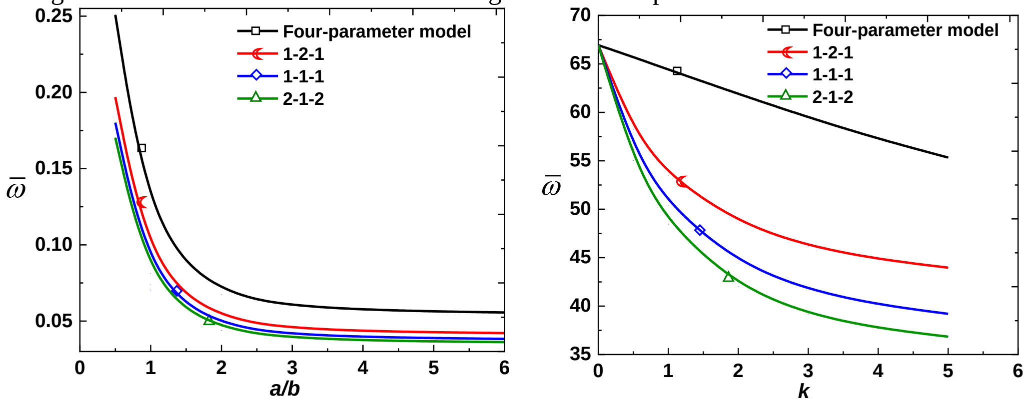

a) b)

Figure 3: Non-dimensional fundamental frequency for FG sandwich and four parameters model plate versus (a): k=2, a/h=10 and (b): a/b=2, a/h=5m a) P-FGSP, b) FP-FGM.

Figure 4a and 4b shows the variation of the non-dimensional fundamental frequency of FG sandwich plate and plate with four parameters model versus the material index "k," which the Al/Al2O3 is used in (a) and Al/ZrO2 used in (b). It can be seen that with increasing index k, the fundamental frequency is rapidly decreased in the case of Fig. 4a. In contrast, the fundamental frequency decreased slower in the case of Fig. 4a. The four parameters model always have the maximum values of the fundamental frequency. So, the variation of index k influence on the stiffness of the plate. The increase in the index k reduced the stiffness of the plate.

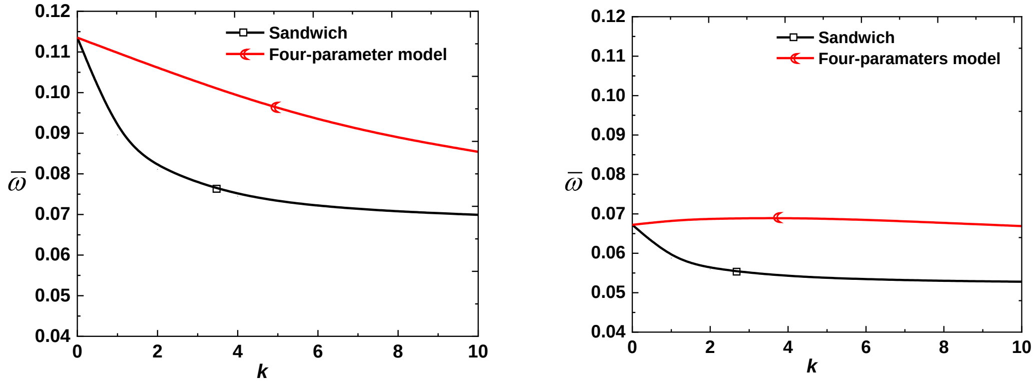

a) b)

Figure 4: Non-dimensional fundamental frequency of square FG sandwich (1-2-1) and four parameters model with two type of FG materials (a): Al/Al2O3 and (b): Al/ZrO2 with a/h= 10a) P-FGSP, b) FP-FGM.

Figure. 5 depicts the variation of non-dimensional fundamental frequency for three modes of FG sandwich and four parameters model subjected on simply supported boundaries for (k=1 and a/h=10). The non-dimensional fundamental natural frequency decreases with the increasing side ratios to thickness (a/h). The four parameters model has the highest value with every single mode.

The non-dimensional fundamental frequency variation of the supported FG sandwich and four parameters model square plate are presented in **Figure. 6a, and 6b** versus the side ratios to thickness (a/h) for various values of material index k are considered. With the increasing of ratios, a/h, the fundamental frequency increased, and then take values approach before a/h=20, the natural frequency end to keep a more constant shape. The ceramic material takes the maximum frequency values, as shown in both figures. In other words, the frequencies decrease as the power law index k increases.

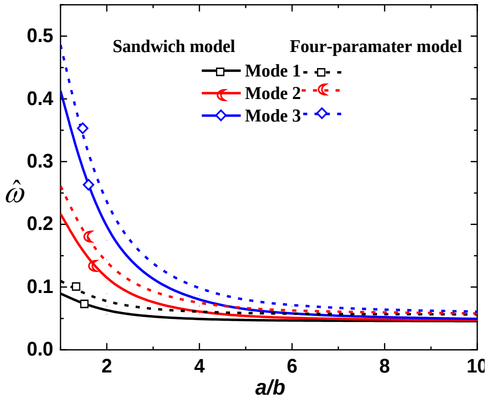

Figure 5: Comparison between non-dimensional fundamental frequency for three modes of FG sandwich and four parameters model (k=1 and a/h=10).

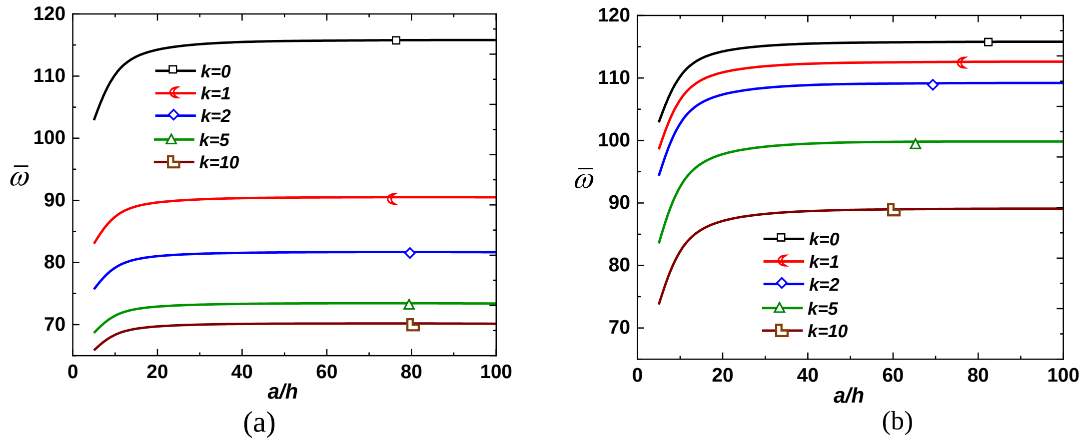

Figure 6: Non-dimensional fundamental frequency for FG square sandwich plate in (a) and plate with four parameters model in (b) versus side to thickness a/h with various values of index k

5. Conclusions

The present article studies and analyzes the free vibration response of simply supported FG plates with four-parameter power law distribution and multi-layered plates using a novel warping function. The formulation used in this work is based on a quasi-3D shear deformation model accounting for integral terms and including the stretching effect. The equations of motion have been derived via Hamilton's principle. The fundamental frequencies were obtained after solving the problem by Navier solution. Effects of volume fraction index k, geometric parameters, and anisotropic ratio on the response of FG sandwich and single layered plate with a four-parameter model are discussed in detail.

According to the results of the study, the following can be drawn:

- The four parameters model always has the high frequencies
- The power law index k influences the variation of frequencies. The stiffness of the plate is reduced when the index k increases.
- The quasi-3D theory is essential for thick, moderately thick FG plates and should be considered in future studies.
- The numerical results have shown the effect of the power-law exponent, the power-law distribution choice, and the choice of the four parameters on the dynamic response of the FG plate considered.

References

[1] S. Zghal, N. Joueid, F. Tornabene, R. Dimitri, M. Chrigui, F. Dammak, Time-dependent deflection responses of FG porous structures subjected to different external pulse loads, *Journal of Vibration Engineering & Technologies*, Vol. 12, No. 1, pp. 857-876, 2024.

[2] A. Heinlein, A. Klawonn, M. Lanser, J. Weber, Combining machine learning and domain decomposition methods for the solution of partial differential equations—A review, *GAMM-Mitteilungen,* Vol. 44, No. 1, pp. e202100001, 2021.

[3] J. A. Palacios, R. Ganesan, Dynamic response of single-walled carbon nanotubes based on various shell theories, *Journal of Reinforced Plastics and Composites,* Vol. 38, No. 9, pp. 413-425, 2019.

[4] S. K. Jena, S. Chakraverty, V. Mahesh, D. Harursampath, Application of Haar wavelet discretization and differential quadrature methods for free vibration of functionally graded micro-beam with porosity using modified couple stress theory, *Engineering Analysis with Boundary Elements,* Vol. 140, pp. 167-185, 2022.

[5] M. D'ottavio, A. Krasnobrizha, E. Valot, O. Polit, R. Vescovini, L. Dozio, Variable Kinematics Models for Advanced Composite Plates, in *Proceeding of,* Springer, pp. 23-34.

[6] A. Neves, A. Ferreira, E. Carrera, M. Cinefra, C. Roque, R. Jorge, C. M. Soares, Static, free vibration and buckling analysis of isotropic and sandwich functionally graded plates using a quasi-3D higher-order shear deformation theory and a meshless technique, *Composites Part B: Engineering,* Vol. 44, No. 1, pp. 657-674, 2013.

[7] A. Tamrabet, B. Mamen, A. Menasria, A. Bouhadra, A. Tounsi, M. H. Ghazwani, A. Alnujaie, S. Mahmoud, Buckling behaviors of FG porous sandwich plates with metallic foam cores resting on elastic foundation, *Structural Engineering and Mechanics, An Int'l Journal,* Vol. 85, No. 3, pp. 289-304, 2023.

[8] F. Tornabene, N. Fantuzzi, M. Bacciocchi, Free vibrations of free-form doubly-curved shells made of functionally graded materials using higher-order equivalent single layer theories, *Composites Part B: Engineering,* Vol. 67, pp. 490-509, 2014.

[9] X. Xie, H. Zheng, G. Jin, Free vibration of four-parameter functionally graded spherical and parabolic shells of revolution with arbitrary boundary conditions, *Composites Part B: Engineering,* Vol. 77, pp. 59-73, 2015.

[10] A. Hajlaoui, E. Chebbi, F. Dammak, Three-dimensional thermal buckling analysis of functionally graded material structures using a modified FSDT-based solid-shell element, *International Journal of Pressure Vessels and Piping,* Vol. 194, pp. 104547, 2021.

[11] R. Ansari, M. Faraji Oskouie, S. Nesarhosseini, H. Rouhi, Nonlinear thermally induced vibration analysis of porous FGM timoshenko beams embedded in an elastic medium, *Transport in Porous Media*, pp. 1-25, 2022.

[12] S. Zghal, D. Ataoui, F. Dammak, Free vibration analysis of porous beams with gradually varying mechanical properties, *Proceedings of the Institution of Mechanical Engineers, Part M: Journal of Engineering for the Maritime Environment,* Vol. 236, No. 3, pp. 800-812, 2022.

[13] S. Kumar, Vibration analysis of Non-uniform axially functionally graded beam resting on Pasternak foundation, *Materials Today: Proceedings,* Vol. 62, pp. 619-623, 2022.

[14] H.-C. Li, L.-L. Ke, Z.-M. Wu, J. Yang, Free vibration of FGM mindlin plates submerged in fluid, *Engineering Structures,* Vol. 259, pp. 114144, 2022.

[15] D. Ouinas, Y. Belkhodja, H. Fekirini, J. V. Olay, B. Achour, M. Touahmia, M. Boukendakdji, A new hybrid HSDT for bending, free vibration, and buckling analysis of FGM plates (2D & quasi-3D), *Smart Structures and Systems, An International Journal,* Vol. 29, No. 3, pp. 395-420, 2022.

[16] V. D. Nguyen, Static bending, free vibration, and buckling analyses of two-layer FGM plates with shear connectors resting on elastic foundations, *Alexandria Engineering Journal,* Vol. 62, pp. 369-390, 2023.

[17] F. Tornabene, E. Viola, Static analysis of functionally graded doubly-curved shells and panels of revolution, *Meccanica,* Vol. 48, pp. 901-930, 2013.

[18] M. Sekkal, B. Fahsi, A. Tounsi, S. Mahmoud, A new quasi-3D HSDT for buckling and vibration of FG plate, *Structural Engineering and Mechanics, An Int'l Journal,* Vol. 64, No. 6, pp. 737-749, 2017.

[19] M. Abualnour, M. S. A. Houari, A. Tounsi, S. Mahmoud, A novel quasi-3D trigonometric plate theory for free vibration analysis of advanced composite plates, *Composite Structures,* Vol. 184, pp. 688-697, 2018.